AD-A229 775

AD-A229 775

REPORT DOCUMENTATION PAGE

DTIC FILE COPY

1a.	1b. RESTRICTIVE MARKINGS
2a. SECURITY CLASSIFICATION AUTHORITY	3. DISTRIBUTION/AVAILABILITY OF REPORT
2b. DECLASSIFICATION/DOWNGRADING SCHEDULE	Unclassified/Unlimited

4. PERFORMING ORGANIZATION REPORT NUMBER(S)	5. MONITORING ORGANIZATION REPORT NUMBER(S)
ONR Technical Report #15	

6a. NAME OF PERFORMING ORGANIZATION	6b. OFFICE SYMBOL (If applicable)	7a. NAME OF MONITORING ORGANIZATION
Dept of Chemical Engineering and Materials Science	Code 1113	Office of Naval Research

6c. ADDRESS (City, State, and ZIP Code)	7b. ADDRESS (City, State, and ZIP Code)
University of Minnesota Minneapolis, MN 55455	800 North Quincy Street Arlington, VA 22217

8a. NAME OF FUNDING/SPONSORING ORGANIZATION	8b. OFFICE SYMBOL (If applicable)	9. PROCUREMENT INSTRUMENT IDENTIFICATION NUMBER
Office of Naval Research		Contract No. N00014-87-K-0494

8c. ADDRESS (City, State, and ZIP Code)	10. SOURCE OF FUNDING NUMBERS			
800 North Quincy Street Arlington, VA 22217-5000	PROGRAM ELEMENT NO.	PROJECT NO.	TASK NO.	WORK UNIT ACCESSION NO

11. TITLE (Include Security Classification)

Measurement of Surface Forces

12. PERSONAL AUTHOR(S)
Christopher P. Smith, Shelly R. Snyder, and Henry S. White

13a. TYPE OF REPORT	13b. TIME COVERED	14. DATE OF REPORT (Year, Month, Day)	15. PAGE COUNT
Technical	FROM 1/1/90 TO 10/31/90	11/16/90	

16. SUPPLEMENTARY NOTATION
Chapter in In-Situ Studies of Electrochemical Interfaces: A Prospectus; H.D. Abruna, ed., VCH Verlag Chemical

17. COSATI CODES			18. SUBJECT TERMS (Continue on reverse if necessary and identify by block number)
FIELD	GROUP	SUB-GROUP	

19. ABSTRACT (Continue on reverse if necessary and identify by block number)

The surface forces apparatus (SFA) described in this chapter is an experimental system for measuring the nature and magnitude of interactions between two surfaces separated by a fluid medium. Applications of the SFA in investigations of polymer structure, solvent ordering at metal and insulator interfaces, hydrodynamic flow in pores, and electrostatic and van der Woods forces (DLVO theory), are described.

20. DISTRIBUTION/AVAILABILITY OF ABSTRACT	21. ABSTRACT SECURITY CLASSIFICATION
☒ UNCLASSIFIED/UNLIMITED ☐ SAME AS RPT ☐ DTIC USERS	Unclassified

22a. NAME OF RESPONSIBLE INDIVIDUAL	22b. TELEPHONE (Include Area Code)	22c. OFFICE SYMBOL
Henry S. White	(612) 625-6995	

DD FORM 1473, 84 MAR   83 APR edition may be used until exhausted.   SECURITY CLASSIFICATION OF THIS PAGE
All other editions are obsolete.

90 12 13 022

CHAPTER 4

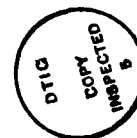# MEASUREMENT OF SURFACE FORCES

Christopher P. Smith, Shelly R. Snyder,
and Henry S. White

Department of Chemical Engineering and Materials Science
University of Minnesota
Minneapolis, MN 55455

CONTENTS

I. INTRODUCTION

The role of electrostatic surface forces in determining the distribution of ions at the electrode/electrolyte interface is well established. However, surface forces also lead to the formation of a number of interesting microscopic structures of current interest to electrochemists. The adsorption of thin layers of redox active polymers onto electrode surfaces, the orientation and density of molecular films, the dispersion of semiconductor particles in photoelectrochemical cells, and the formation of ultra-thin and stable wetting layers necessary for various forms of atmospheric corrosion are a few examples where surface interactions are recognized as playing key roles. Although the characterization of microstructures on electrode surfaces is now possible by various electrochemical and spectroscopic techniques, it has proven generally difficult (and more often not considered) to directly measure the interactions between components that lead to stable systems. The possibility of directly measuring forces at electrode surfaces (and at chemically modified electrode surfaces) is an enticing proposition in that fundamental insights gained in understanding the nature of these interactions may provide clues for predicting interfacial structure.

The surfaces forces apparatus [1] described in this chapter is an experimental system for measuring the nature and magnitude of interactions between two surfaces separated by a fluid medium. The basic measurement developed by Israelachvili and coworkers, and now applied in many research laboratories, consists of bringing two ultra-smooth surfaces (typically, but not limited to, molecular smoothness) together within distances comparable to the decay length of the interaction being measured, e.g., the Debye length. Forces between the two surfaces are measured as a function of the distance separating the surfaces by means of optical and electromechanical measurements (described in detail in section II). Depending on the nature of the surface interactions, the measurements can be made over relatively large distances (e.g., 10 - 1000 Å for electrostatic forces between two electrically charged or ionized surfaces) or short ranges (e.g., <30 Å for structural forces). More often, two or more types of surface forces with different decay lengths can be quantitatively measured in one experiment, resulting in a complete force law describing the surface interactions across the fluid.

A striking result obtained from surface forces measurements that demonstrates the unique cap: / of this experimental

approach is the measurement of the "quantization" of liquids entrapped between mica sheets [2-6] or between mica and an electrically conductive metal film [7]. An oscillatory force vs distance curve [Fig. 1] is observed due to the ordered layering of liquid molecules as the separation of surfaces is decreased below 5 to 10 molecular diameters. Other successes of this technique include experimental verification of the DLVO theory describing
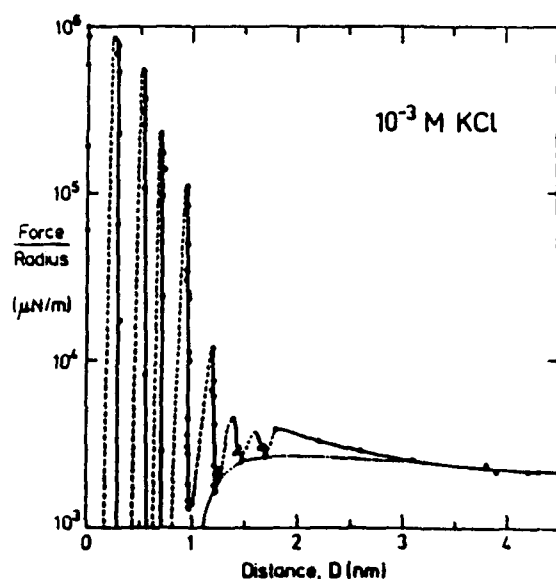

Figure 1. *Force vs. distance measured for mica sheets immersed in 10^{-3} M KCl. The oscillatory force curve below 2 nm is the result of the layering of water between negatively charged mica surfaces, partially neutralized by adsorption of K^+. The surface coverage was estimated to be ca. one K^+ per 1.2 nm^2. The forces beyond 2 nm separation result from the combination of repulsive coulombic forces (described by the Poisson-Boltzmann equation) and attractive van der Waals forces (described by the Hamaker equation). (From Reference 44. Copyright © 1985 Royal Swedish Academy. Reprinted with permission of Cambridge University Press.)*

the combined interactions of van der Waals and electrostatic forces [8], measurements of (a) long range hydrophobic forces [9-11], (b) frictional forces between surfaces separated by molecular distances [12] and (c) forces between surface adsorbed polymers [13-16]. In the past three years, surface forces apparatus techniques have begun to be applied by several research groups to study the interactions between solid metal electrodes separated by an electrolytic solution. Electrostatic forces, which are intimately related to electrode kinetics and adsorption phenomena, have been directly measured between Pt surfaces [17]. In addition, van der Waals [18], solvation [7], and adhesion forces [19] between metal surfaces have been measured by similar techniques.

Although the surface forces apparatus is capable of resolving distances between two surfaces with 1 Å resolution, it is important to note that the forces are being measured between two macroscopic surfaces. Unlike the scanning tunneling microscope [20] in which an atomically sharp tip is brought close to a single surface, no topographical information from force measurements is obtained unless it is inferred *indirectly* from the observed forces (such as in the smearing out of oscillatory forces on an atomically rough surface) [21]. On the other hand, surface properties manifest themselves by such factors as surface electrostatic charge, hydrophobicity, crystallographic orientation [22], and so forth.

In the ensuing sections, selected experimental work is presented demonstrating the use of the surface forces apparatus to measure interactions between insulating and metallic surfaces. The examples have been specifically chosen to emphasize relationships between forces and interfacial structures that are of interest to chemists and especially to electrochemists. Interfacial structure is defined broadly in this account, and includes, for example, the hydration of ionic surfaces as well as the swelling of polymer films. Our coverage is incomplete—recent advances in the understanding of adhesion forces, forces between amphiphilic layers, and frictional forces have been obtained from surface forces measurements. These investigations have had an impact in many areas of science and engineering, but have been judged to be of less interest to the electrochemical community than the topics that were chosen.

The vast majority of force measurements during the 1970s and 1980s were concerned with physical interactions between surfaces of mica; mica can be readily cleaved to yield large area specimens that are molecularly smooth and relatively inert. However, mica

can be modified with metallic, polymeric, semiconductor, or surfactant overlayers or replaced entirely with other molecularly smooth surfaces, e.g., highly oriented pyrolytic graphite [19]. The study of chemical and physical interactions between these different materials is the direction that many laboratories are now pursuing.

II. SURFACE FORCES APPARATUS AND MEASUREMENT THEORY

The surface forces apparatus developed and popularized by Israelachvili [1,23] [Fig. 2] will form the basis for our description of the basic principles of force measurements. This instrument provides the only direct method by which forces within the electrode/electrolyte interface can be measured as a function of distance, anywhere from thousands of angstroms to contact with a distance resolution of ca. 1 Å. The technical requirements of the measurement are:

1. Surfaces sufficiently smooth to permit meaningful measurements;
2. A method to move the surfaces together in angstrom increments;
3. A method of measuring the separation distance between surfaces.

A. General Description

The entire apparatus is constructed of 316 stainless steel, glass, and other inert plastics or polymers such as Teflon and Kel-F. Two molecularly smooth mica samples are mounted on hemicylindrical glass supports (radius ~ 2 cm) and oriented with respect to each other in a crossed-cylindrical geometry to allow a number of possible contact positions. The lower support is secured to a weak cantilever spring which is attached to a spring assembly; the upper is secured to a plate which is contacted by a piezoelectric tube.

The surfaces mounted on the glass supports can be moved toward or away from each other in three ways. The spring assembly accomplishes a course and fine adjustment of separation distance through the motions of two micrometer rods. The upper rod is controlled by a stepper motor and is used before an experiment to coarsely adjust the surface separation. The lower
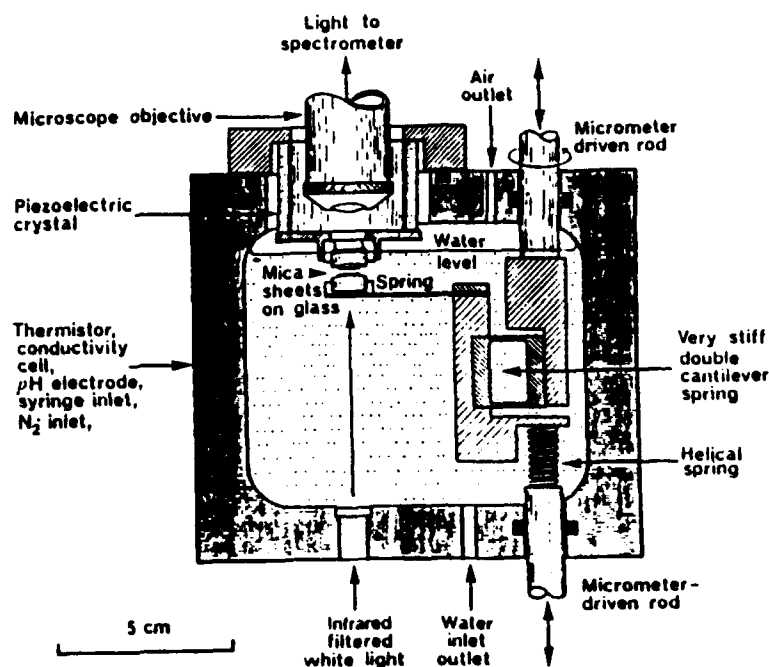
Figure 2. *Schematic drawing of surface forces apparatus developed by Israelachvili. (Reprinted by permission from Nature 262: 774. Copyright © 1976 Macmillan Journals Limited.)*

rod is driven by a synchronous motor which affects the surface separation through a coupled spring assembly. The difference in force constants of the helical and double cantilever spring allows for a thousand-fold reduction in motion, so that a micron change in rod height is reduced to a nanometer change in surface separation. Finest adjustments of surface separation are made with the piezoelectric tube, which drives the upper surface. With a 1 nm/V expansion coefficient, separations can be controlled to within 1 Å.

The changes in surface separation are measured by optical interferometry [24]. A tungsten-halogen lamp provides an intense source of white light, which is collimated, IR filtered (to reduce heating of the apparatus), and directed to the surfaces. As it passes through the surfaces, multiple reflections take place between silver layers that are deposited onto the backsides of the

mica before mounting. This results in the constructive and destructive interference of certain wavelengths over others. The transmitted intensity profile is focused and directed to a spectrometer where it is viewed as an array of fringes that correspond to the wavelengths of constructive interference. The shape, position, and separation of these fringes is uniquely determined by the refractive index and physical thickness of the materials through which the light passes.

The force acting between the surfaces is determined by measuring deflections in the single cantilever spring which supports the lower mica surface. These deflections are measured using the optical system and, when multiplied by the spring constant (~100 N/m), yield the force acting between the surfaces with a sensitivity of about 10 nN (10 μg).

In all experiments great care is taken to ensure the mechanical stability of the system through vibration isolation and thermal control. Dust particles are avoided by performing all preparatory work in a laminar flow hood and by filtering all fluids that enter the apparatus.
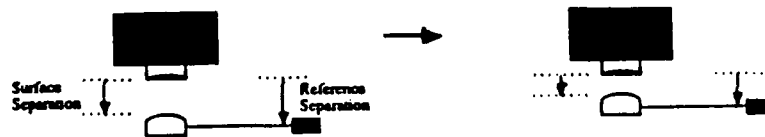
B. Force Measurement

To measure the force acting between the two surfaces, one must measure the deflections in the force measuring cantilever spring that holds the lower glass support. Since these deflections are only on the order of angstroms, conventional techniques of measuring displacement, e.g., a traveling microscope, are of no use. Instead, the mechanical displacements of the surfaces are monitored with optical interferometry. The combination of mechanical and optical methods allows one to deduce deflections to within a few angstroms. For example, pushing against the coupled spring assembly with the lower micrometer rod (as described above) is one method of controlling the separation between the surfaces. Displacements of the rod are monitored by using a high precision linear potentiometer attached to the synchronous motor which drives this rod.

At a distance where no forces are encountered (several thousand angstroms), a calibration curve is started by recording the initial separation distance and resistance across the potentiometer. Subsequent distances and resistances are recorded point by point as the surfaces are driven together. The calibration curve of distance D vs resistance ρ is a straight line with slope $dD/d\rho$. The theoretical change in surface separation may be computed by multiplying the change in potentiometer resistance

$\Delta\rho$ by the proportionality constant $dD/d\rho$ given by the calibration. As long as no forces are acting between the surfaces, the change in reference separation ΔD_{ref} is equal to the change is surface separation measured optically ΔD_{surf} [25]. Once forces are encountered, the optically measured change in surface separation is greater or less than the reference change in separation predicted from the calibration [Fig. 3]. The difference in these two values,

$$\text{Force} = K \cdot \text{Spring Deflection} = K \cdot \left[\Delta \begin{smallmatrix} \text{Surface} \\ \text{Separation} \end{smallmatrix} - \Delta \begin{smallmatrix} \text{Reference} \\ \text{Separation} \end{smallmatrix} \right]$$

Figure 3. *Schematic description of force calculation (From Reference 25, with permission.)*

the spring deflection, is multiplied by the force constant of the spring K to yield the force between the surfaces (i.e., Hooke's law):

$$\text{Force} = K \cdot \text{spring deflection} = K \cdot [\Delta D_{surf.} - \Delta D_{ref.}]. \quad (1)$$

The sign of the force is positive or negative depending on whether the surface forces are repulsive or attractive, respectively. The spring constant may be calibrated independently by adding known masses to the spring and measuring the deflection, e.g., via a reflected laser beam. The error in measuring K ($\leq 1\%$) sets the limit on the accuracy of the forces measured.

It is worth mentioning here that the forces measured with the crossed-cylinder configuration can be related to the theoretically more tractable geometry of parallel planes through an approximation first proposed by Derjaguin [26,27]. The force between two crossed cylinders, F_{cc}, at a given nearest separation is related to the energy of interaction per unit area of two parallel plates, E/A_{pp}, at the same separation through a geometric factor, G.

$$F_{cc} = G \cdot (E/A)_{pp} \quad (2)$$

For two cylinders of radius r_1 and r_2 crossed at an angle of ω, G is $2\pi\sqrt{(r_1 r_2)}/\sin \omega$. For cylinders of equal radii, R, crossed at 90°, G is $2\pi R$. It is customary to report forces normalized by the radius, F/R, to facilitate the comparison of experimental results obtained in different laboratories.

C. Optical System and
Multiple-Beam Interferometry [24]

When the mica surfaces are in contact, the light reflected between the silver layers on the backsides of the mica develops a profile of constructive and destructive interference. This interference pattern is focused and directed to a spectrometer where the constructively transmitted wavelengths are viewed as a set of "fringes of equal chromatic order" (FECO) [Fig. 4].

The position of these fringes is measured with a ruled microscope objective that is mounted on a translating micrometer stage. This stage is calibrated with the mercury green ($\lambda = 5460.7$ Å) and doublet yellow ($\lambda = 5769.6$ or 5790.6 Å) emission lines, yielding a wavelength to displacement ratio of ~ 32 Å/mm. The smallest measurable step of the stage is 1 μm and under optimal conditions, measurements of the fringe wavelength can be made to
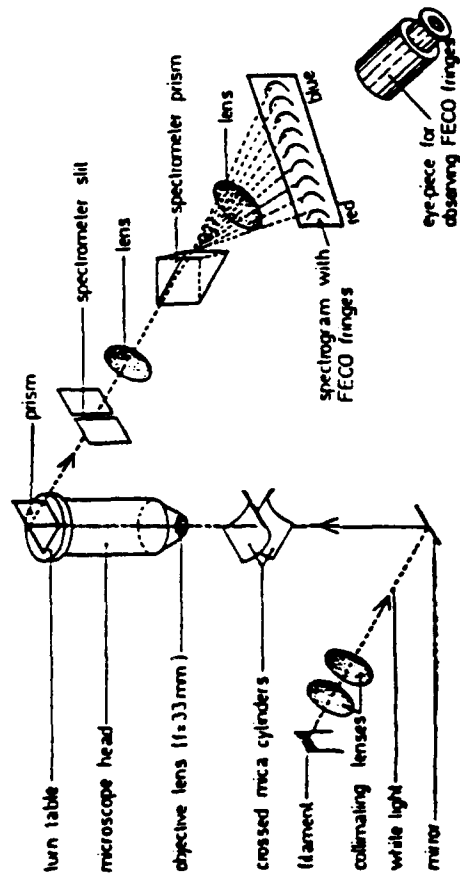
Figure 4. *Schematic of optical system used to measure fringes of equal chromatic order (FECO). (From Reference 28, with permission.)*

within 0.1 Å.

The exact position of the fringes when the surfaces are in *direct contact* depends on the mica's refractive index μ_{mica} and its physical thickness T_{mica}. Those rays with wavelengths that exit the Ag/mica/mica/Ag interferometer in phase are the wavelengths that produce the fringes in the spectrometer and satisfy the equation

$$\lambda_m^0 = \frac{2\mu_{mica}(D_{mica})}{m} \; ; \; m = 1,2,3,... \; ; \; D_{mica} = 2T_{mica}, \quad (3)$$

where the superscript "0" refers to the fringe wavelength when the surfaces are in contact and the subscript "m" identifies the fringe number. Any two successive wavelengths, λ_m^0 and λ_{m-1}^0 allow one to calculate the fringe number and the mica thickness when the refractive index of mica is known [28].

When the surfaces are separated to a distance D, the optical path length increases, and the wavelengths that pass constructively between the interferometer shift correspondingly toward longer wavelengths: $\Delta\lambda_m = \lambda_m - \lambda_m^0$. These shifts are used to calculate the separation distance between the surfaces:

$$D = \frac{m \, \Delta\lambda_{m(odd)}}{2\mu_{mica}} \quad m = 1,3,5,... \quad (4)$$

$$D = \frac{m\mu_{mica} \, \Delta\lambda_{m(even)}}{2 \, \mu_{med}^2} \quad m = 2,4,6,.... \quad (5)$$

Due to the different dependence of the fringe orders (odd, even) on the refractive index of the medium, μ_{med}, these two equations can be solved simultaneously to give the separation distance between the mica surfaces *and* the refractive index of the intervening medium.

Equations (4) and (5) are good approximations for $\Delta\lambda_m/\lambda_m^0 \ll 1$ and suffice to demonstrate the accuracy possible with the method. For $m = 22$ (corresponding to 2 μm thick mica sheets), $\mu_{mica} = 1.58$, and $\mu_{med} = 1.33$ (water), $\partial D \approx 10 \, \partial(\Delta\lambda_m)$. Under optimum conditions with the uncertainty in $\Delta\lambda_m$ equal to 0.1 Å, the uncertainty in D is about 1 Å or less. Factors which significantly alter the accuracy of the measurement include nonlinear dispersion [28] and the introduction of reflective overlayers on the mica [29]. An effect of the latter is depicted in Figure 5 where the even order fringes are obscured by reflections between the Ag and Pt layers.
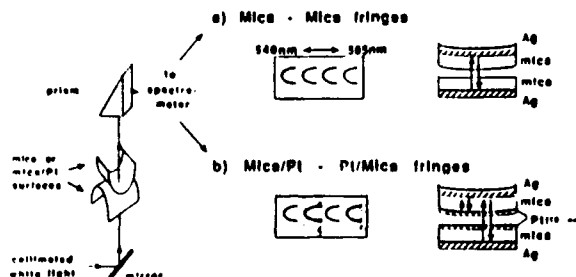
Figure 5. *Qualitative features of the FECO observed for mica and Pt coated mica surfaces. (Reprinted with permission from Reference 17. Copyright © 1988 American Chemical Society.)*

III. ELECTROSTATIC AND VAN DER WAALS FORCES

The earliest and most extensive studies of surface interactions were concerned with verification of theories describing repulsive electrostatic and attractive van der Waals forces. The combination of these opposing forces, described by the DLVO theory [30,31] (named after Derjaguin, Landau, Verwey, and Overbeek), is the basis of a variety of common phenomena, e.g., adhesion, the equilibrium thickness of soap films, and the stabilization of colloidal suspensions. In 1959, Derjaguin and coworkers, at the Academy of Sciences in Moscow, published an account [32,26] of the measurement of electrostatic forces between two smooth, 300 μm diameter Pt wires, oriented in a crossed cylindrical fashion and immersed in various aqueous and nonaqueous electrolytes. Their instrument was the forerunner of the present day surface forces apparatus, and the results they obtained caught the attention of at least one prominent electrochemist. In a 1960 review article [33] of the ionic double layer at metal surfaces, A. N. Frumkin included a part of Derjaguin's results [Fig. 6] showing the magnitude of the force barrier surmounted while bringing two Pt wires to electrical contact as a function of their potential (measured vs a calomel electrode). These curves and ones obtained in other electrolytes show a pronounced minimum in the force vs potential curve at low ionic concentrations
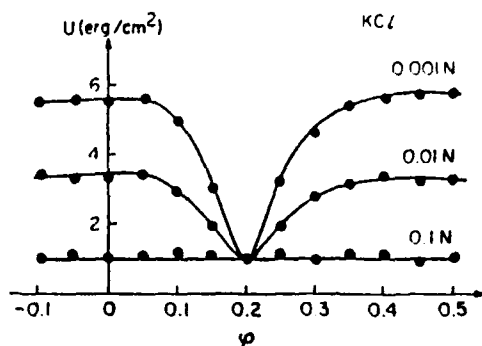
Figure 6. *Energy barrier surmounted in bringing two 300 µm diameter Pt wires together to electrical contact as a function of potential. The Pt wires were poised at the same potential (φ) referenced to a calomel electrode. (From Reference 26, with permission.)*

(corresponding to the potential of zero charge of Pt) and a potential independent force at high concentrations, qualitatively similar to capacitance curves observed for many liquid metals. Frumkin wrote:

> It is not quite clear why in this case [*viz.* surface forces measurements] we do not meet with the difficulties, which were encountered during the attempts to determine the location of the zero charge potential of platinum from the capacity minimum in dilute solutions [33].

Frumkin's early report is of some historical interest, since the technique of measuring forces was apparently not applied again to electrochemical studies until the mid 1980s; his comment also clearly points out an important advantage of surfaces forces measurement techniques applied to the study of solid electrodes. The difficulties in measuring the capacitance of Pt electrodes, referred to by Frumkin, resulted from dispersion of interfacial capacitance due to roughness and other surface heterogeneities and from psuedocapacitances arising from adsorption of hydrogen and oxygen. The force barrier, as correctly analyzed by Derjaguin,

clearly resulted from the repulsion between surfaces as their diffuse double layers overlapped at close separation. The diffuse distribution of ions surrounding the electrode held near the potential of zero charge, however, was not influenced as strongly by microscopic roughness or by the adsorption of solutes. Thus, the potential of minimum electrostatic force in dilute solutions, analogous to a capacitance minimum at the p.z.c., was more readily apparent.

In Derjaguin's measurements, the roughness of the Pt wires limited quantitative determination of the separation distance to several hundred angstroms and greater; thus, the shape of the electrostatic force curve at shorter distances was not determined. The measurements of Tabor and Winterton in 1968 [34] of normal and retarded van der Waals forces between layers of cleaved muscovite mica separated by air was the first direct measurement of forces at separations below 100 Å. Besides first recognizing the utility of mica as a necessary ultra-smooth substrate for measuring short-range interactions, their experimental ap￢ ￢atus also made use of a piezoelectric transducer to vary the ser ￢tion distance, and multiple beam interferometry (using fringes of equal chromatic order) to measure the separation distance, both of which are essential elements of the apparatus employed by most researchers today. Although fused silica and various polished glasses have been employed subsequently, mica has remained the most common choice for surface forces apparatus measurements, being used either as a bare surface or as a substrate modified by the deposition of optically transparent metal, surfactant or polymers films.

The surface forces apparatus has been employed by Israelachvili and coworkers in detailed studies of DLVO forces between bare mica surfaces immersed in aqueous electrolytes [35,1]. A general conclusion of their work is that the Poisson-Boltzmann equation and the Liftschitz theory of van der Waals interactions give good quantitative predictions of the observed forces in solutions containing symmetrical electrolytes for separations down to ca. 20 Å. Other types of forces, however, are often dominant below this distance, as will be discussed below.

Before considering the experimental observations, it is worth noting some of the chemical properties of mica. The dissociation of K^+ gives the surface of mica a net negative charge, creating an electrical double-layer whenever a bare mica surface is in contact with an aqueous solution. The mica/electrolyte double-layer

structure is analogous to what electrochemists imagine exists at metal/electrolyte interfaces [36]. The force measurements unequivocally demonstrate a diffuse double-layer region, as well as a "compact" layer that is analogous to, but far more *structurally* complex than, the simplified picture that is generally drawn of the inner and outer Helmholtz layers. In nonaqueous solutions, e.g., cyclohexane, and in the absence of additional electrolyte, K^+ ions remain adsorbed onto the surface, and electrostatic forces are correspondingly absent. The notable and obvious difference between mica and metal surfaces is that mica is an excellent electrical insulator. Two consequences of this factor are that (a) the charge on the crystal surface, resulting from ionization, is spatially localized, and (b) the net charge per unit surface area in any particular experiment is determined and fixed by chemical interactions with the solution (e.g., adsorption of ions). The latter factor limits the measurement of forces to a relatively small range of surface potential ($<$ |150 mV|) in comparison to what is possible with electrochemical systems. Cleaved mica, however, has a sufficiently high surface charge density (0.5 negative charges/nm^2) that it is generally assumed in analyzing force curves that one is dealing with a surface of uniform charge.

Figure 7 schematically shows the interactions energy between two surfaces based on the DLVO theory [8]. The total energy (solid line) can be considered as the sum of the van der Waals and electrostatic interactions (broken lines). The electrostatic force between *identical* surfaces is always repulsive, regardless of distance, and acts in the presence of attractive van der Waals dispersion forces. However, the exact shape of the interaction profile depends markedly on the solution composition. In air (or vacuum) or in non-polar solvents without added electrolyte, the electrostatic contribution is negligible relative to the van der Waals interaction and the measured forces between surfaces are attractive. In polar liquids containing a small concentration of ions, the electrostatic contribution is large, and repulsive double-layer forces can be measured from contact out to separations of 0.1 μm and beyond. At higher ionic concentrations (e.g., 1 M KNO_3), the Debye screening length (κ^{-1} = 0.3 nm) shortens to distances comparable to values over which van der Waals interactions occur, resulting in a complex force curve which may exhibit both local maxima and minima [Fig. 7].

Figure 8 shows force vs distance curves obtained by Israelachvili and Adams [1] for two mica layers separated by KNO_3 solutions of various concentrations. The forces shown in
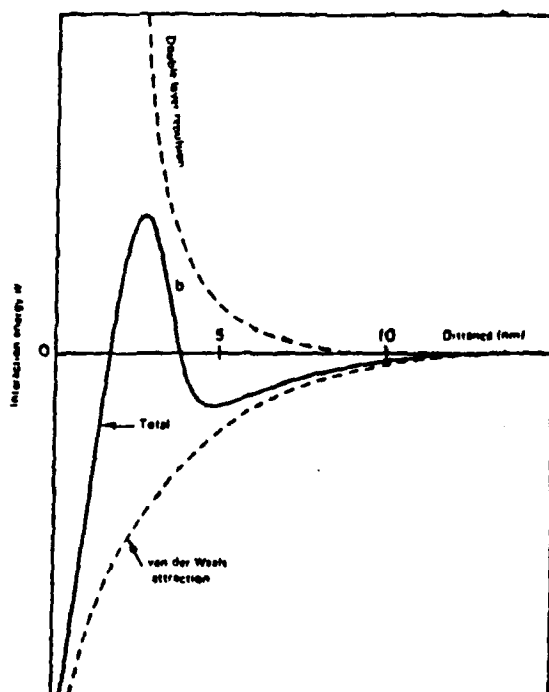
Figure 7. *Schematic representation of the interaction energy* W *as a function of distance between two surfaces. The total surface interaction (solid line) is the sum of the attractive van der Waals and repulsive electrostatic interactions (dotted lines). The maximum in the interaction energy shown schematically at ca. 3 nm corresponds qualitatively to the barrier between two Pt surfaces measured by Derjaguin [e.g., Fig. 6]. (From Reference 8, with permission.)*
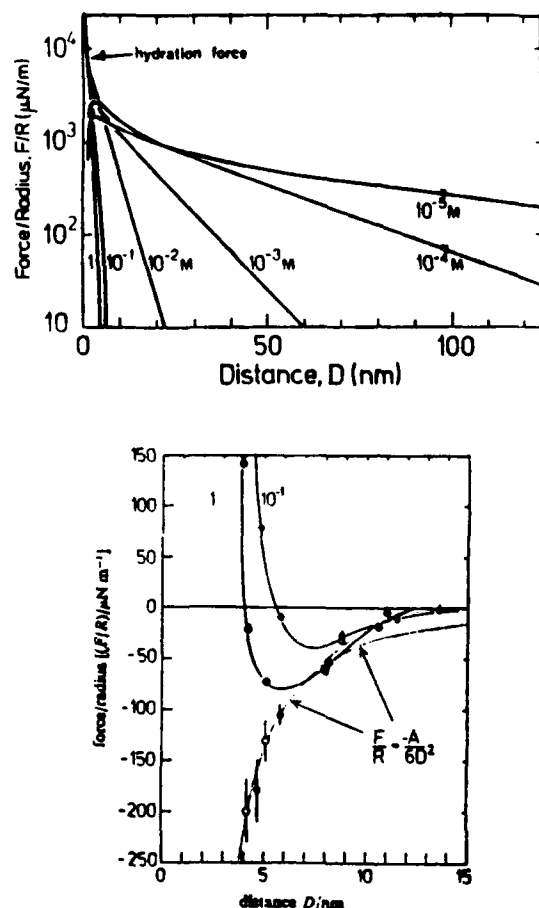
Figure 8. *(top) Repulsive electrostatic forces as a function of distance between mica in aqueous solutions containing 10^{-5} to 1 M KNO_3 (From Reference 44. Copyright © 1985 Royal Swedish Academy. Reprinted with permission of Cambridge University Press); (bottom) DLVO forces (solid circles) as a function of separation distance in 0.1 and 1 M KNO_3. Open circles represent the resulting forces after subtraction of the electrostatic component. The dashed line represents the inverse square van der Waals force law, using a Hamaker constant of A = 2.2 x 10^{-20} Joules. (From Reference 1, with permission.)*

Figure 8 (top) at distances greater than 20 Å are long-range repulsive forces resulting from the overlapping surface double-layers. (In this and all other figures, repulsive forces are plotted as positive values and attractive forces as negative values.) These force profiles may be analyzed by fitting the linear portions of the curves to an analytical expression which is a function of the Debye length, κ^{-1}, and the surface potential, ψ_0. The analysis of electrostatic forces in this region is straightforward. The objective is to describe the variation of pressure between two planar surfaces (a much simpler geometry than crossed cylinders) as a function of distance. Once this is known, the pressure may be integrated with respect to distance to give the interaction energy per unit area, E/A. Then, using the Derjaguin approximation [Eq. (2)], this energy for two planar surfaces is converted directly to the force between the two hemicylindrical surfaces. The derivation is based on the assumption that the potential distribution is governed by the Poisson-Boltzmann (P-B) equation which, in cgs units, is

$$\frac{d\psi^2}{dx^2} = \frac{-4\pi e}{\varepsilon} \sum_i z_i n_i^0 \exp(\frac{-z_i e \psi}{kT}), \qquad (6)$$

where ψ is the potential which varies with distance x in a medium with dielectric constant ε. The summation gives the charge density, which is composed of all ionic species in the medium (subscript "i") which have bulk concentration n_i^0 and valency z_i. The constants e, k, and T are the electronic charge, Boltzmann constant, and the absolute temperature, respectively.

The electrostatic contribution to the pressure between two planar surfaces is a result of the excess osmotic pressure of the ions at the midpoint between the two planes:

$$P = kT \ (\Sigma_i n_i^m - \Sigma_i n_i^0). \qquad (7)$$

The summations give the total ionic concentrations at the midplane (superscript "m") and in the bulk (superscript "0"). Both of these values are given by the Boltzmann equation

$$n_i^x = n_i^0 \ \exp(-z_i e \psi_x/kT), \qquad (8)$$

which describes how the ion concentrations vary from a value of n_i^0 in the bulk (where the potential is assumed equal to 0) to a greater or lesser concentration as the ions are attracted or repelled by the electric field extending from the surface.

For a symmetrical electrolyte at a bulk concentration of n^0 the values of n_i for the anion, $z_i = -z$, and cation, $z_i = +z$, evaluated at the midplane potential, $\psi = \psi_m$, and the bulk potential, $\psi = 0$, may be evaluated with Equation (8) and substituted into Equation (7) to yield

$$P = 2n^0kT \left[\cosh(ze\,\psi_m/kT) - 1\right], \qquad (9)$$

the cosh term arising from the identity $e^x + e^{-x} = 2\cosh x$.

Equation 9 will give the desired relationship between the pressure and separation distance once the variation of the midplane potential is defined with respect to distance. Ideally, this would be accomplished by solving the Poisson-Boltzmann equation between two planar walls [37]. Although there is no analytical solution for this problem, it is possible to obtain an approximation for distances greater than the Debye length by superimposing the potential distributions from each of two such isolated surfaces that face each other in a parallel plane geometry [38]. These potential profiles are obtained by solving Equation (6) with the appropriate boundary conditions, e.g., assume that the surface potential is fixed so that $\psi(x = 0) = \psi_0$ and $\psi(x = \infty) = 0$, to yield

$$\gamma = \gamma_0 \exp(-\kappa x), \qquad (10)$$

where $\gamma = \tanh(ze\,\psi/4kT)$ and $\kappa^{-1} = \dfrac{4\pi e^2 \Sigma_i z_i^2 n_i^0}{\varepsilon kT}$.

At distances greater than the Debye length, the potential will be small, regardless of the potential at the surface, so that the left-hand side of Equation (10) may be replaced with $ze\,\psi/4kT$ and rearranged to give an expression for the potential

$$\psi = \frac{4kT\gamma_0}{ze} \exp(-\kappa x). \qquad (11)$$

Assuming that such profiles extend from each of the two parallel faces, the value of the potential at the midplane (where x is half of the separation distance, $D/2$) is given by the supposition of the profiles:

$$\psi_m = \frac{8kT\gamma_0}{ze} \exp(-\kappa D/2). \qquad (12)$$

This is substituted into Equation (9) and, because this value of ψ_m was obtained under the assumption of small ψ, the cosh term may

be replaced with the leading terms of the power series expansion ($\cosh x = 1 + x^2/2! + x^4/4! + ...$). This yields an expression for the pressure in terms of the Debye length and the surface potential:

$$P = 64n^0 kT\gamma_0^2 \exp(-\kappa D). \tag{13}$$

Equation (13) may be integrated with respect to distance to give the desired interaction energy per area between the planar surfaces. To obtain this energy for surfaces at a separation of D, the integration is performed from infinite separation (where the pressure is zero) to D to yield

$$E/A = (64n^0 kT/\kappa)\gamma_0^2 \exp(-\kappa D). \tag{14}$$

The final step in the analysis is to relate this energy to a force between the hemicylindrical surfaces (i.e., Derjaguin approximation [Equation (2)] by noting that $E/A = F/2\pi R$. Since κ^{-1} is defined by the solution composition and temperature, the only adjustable parameter is the surface potential, ψ_0.

From the foregoing analysis, a plot of $\ln(F/R)$ vs D is expected to be linear, with a slope proportional to κ^{-1} and an intercept related to the surface potential ψ_0. Figure 8 (top) bears out the linearity of $\ln(F/R)$ vs D for mica separated by KNO_3 solutions over several Debye lengths, and Table 1 presents κ^{-1} and ψ_0 values determined by this procedure.

Despite some uncertainty in the exact value of ψ_0 resulting from variations in the chemical composition (% weight K^+) of different mica samples [1], the measured electrostatic repulsive forces between mica separated by dilute symmetrical electrolytes appear to be well described by the Gouy-Chapman theory. Under

TABLE 1. Debye Length and Surface Potential as a Function of Electrolyte Concentration[a]

$[KNO_3]$	κ^{-1} *(theory)*	κ^{-1} *(expt.)*	ψ_0 *(expt.)*
10^{-1} M	9.6 Å	11.5 Å	75 mV
10^{-2}	30	37.5	62
10^{-3}	96	99	85
10^{-4}	304	291	82

[a]*Data taken from Reference 1.*

other conditions, there are significant discrepancies between experiment and theory. In high concentrations of KNO_3, e.g., 1 M, κ^{-1} values are ~25% higher than theoretical values, and it is necessary to assume that the outer Helmholtz plane is shifted to ~2.5 nm beyond the surface in order to obtain a finite value for the surface potential. This phenomenon is now understood to result from hydration forces (or solvation forces) resulting from the structural ordering of H_2O between the surfaces and the hydration of adsorbed K^+ on the surface.

In nonsymmetrical electrolytes containing a divalent ion, e.g., $Ca(NO_3)_2$, κ^{-1} is much smaller (20-45%) than anticipated, signaling a reduction in the extent of repulsive electrostatic forces. This apparent reduction is believed to be the result of an ion correlation effect, which has only recently been theoretically predicted to occur between highly charged surfaces in solutions of high charge density [39], e.g., in solutions containing divalent ions. In essence, this effect arises because the local ion distribution not only reflects the average or mean-field imposed by the screened surface charge, but also the field imposed by other ions in solutions; i.e., there is a correlation between ions that is not accounted for by the Gouy-Chapman theory. The importance of ion-correlation effects on electrochemical double-layer structures has not been experimentally investigated to our knowledge, but appears significant enough to warrant investigation.

Van der Waals forces can be observed in aqueous KNO_3 solutions at close separations and at high ion concentrations. For example, if the force curves in Figure 8 (top) for 0.1 and 1 M KNO_3 are plotted in more detail at distances below 20 nm [1], there is a small but significant attraction between the surfaces, and the force curves pass through a distinct minimum [Fig. 8 (bottom)]. These attractive forces have been attributed to van der Waals dispersion forces, which in theory are essentially independent of the electrolyte concentration. To demonstrate this, Israelachvili and Adams mathematically subtracted electrostatic forces, extrapolated from measurements made at large separations, from the total observed forces at short ranges. The remaining van der Waals forces obtained in 0.1 and 1.0 M KNO_3 solutions were found to coincide, in agreement with theory. Further, by using an inverse square law for the force ($F/R = -A/6D^2$ where the Hamaker constant $A = 2.2 \times 10^{-20}$ J), these authors found good quantitative agreement between the experiment and nonretarded van der Waals theory.

In our laboratory, we have measured repulsive electrostatic forces between optically transparent Pt films deposited on mica [17]. These results are very preliminary, but they demonstrate that short-range forces at solid electrodes can be measured at distances comparable to those obtained using mica. Figure 9 shows the force vs distance curve obtained for two identical 4 nm thick Pt electrodes immersed in H_2O. Measurable forces are observed beginning at about 16 nm and increase approximately exponentially with decreasing separation. Typically, the closest approach of the two surfaces is about 1 nm ($D = 0$ corresponds to contact in air). That the surfaces apparently "contact" at distances greater than expected may be due to surface asperities. However, it is noteworthy that a 1 nm distance of closest approach is in reasonable agreement with the surface roughness estimated from scanning tunneling microscopy [40] [Fig. 10]. This surface roughness complicates interpretations of the interaction between metal layers at very short distances.

From electron diffraction and transmission electron microscopy, the Pt films are known to be polycrystalline, with an approximate average grain size of 20 Å or less, which is considerably smaller than the total interaction area between the crossed cylindrical surfaces. Thus, the measurements we have made result from interactions between numerous grains with different crystallographic orientations. Calculated force curves, using the nonlinear Poisson Boltzmann equation to describe the forces [41], are in good agreement with the data. Average values of $|\psi_0| = 51 \pm 13$ mV and $\kappa^{-1} = 65 \pm 22$ nm were obtained from a set of independent measurements in H_2O. The screening length κ^{-1} is much shorter than expected for pure H_2O and corresponds roughly to an impurity ion concentration (1:1 electrolyte) of 10^{-5} M. The reasonable agreement between the experimental and measured force curves has led us to believe that the excess surface charge is associated with ionized surface-adsorbed species or to localized charge induced in the film during sputter deposition.

IV.- STRUCTURAL FORCES [42]
AND HYDRODYNAMIC FLOW

As mentioned in the preceding section, the DLVO theory fails to adequately predict the repulsive short-range forces observed between mica layers immersed in concentrated KNO_3 solutions. This phenomenon is not specific to KNO_3; similar discrepancies
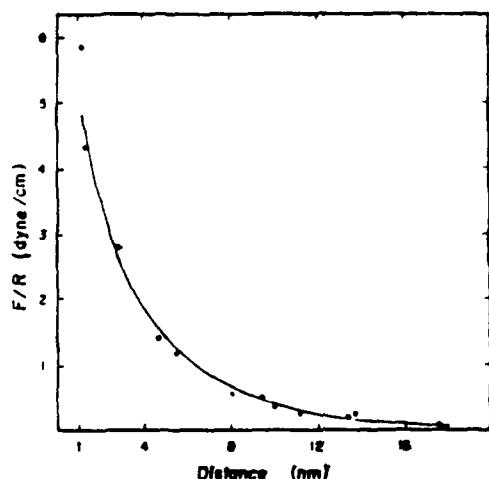
Figure 9. *Force versus distance for Pt coated mica surfaces separated by water. The solid line represents the best fit of the data using the non-linear Poisson-Boltzmann equation. (Reprinted with permission from Reference 17. Copyright © 1988 American Chemical Society.)*
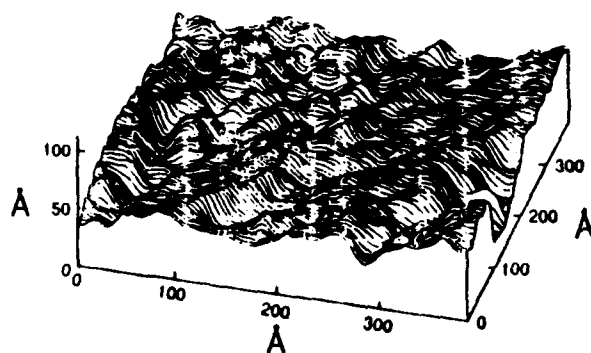

Figure 10. *Scanning tunneling microscope image of 40 Å thick Pt film r.f. sputtered deposited on cleaved mica. (Reprinted with permission from Reference 40. Copyright © 1989 American Chemical Society.)*

between fluid-based continuum theories and experimental force measurements at very small separations have been measured in aqueous solutions containing various electrolytes, and in a number of nonpolar organic solvents, for example, cyclohexane and n-hexadecane [5]. The consensus of laboratories studying these interactions is that these discrepancies are the effect of an additional force (or forces) resulting from hydration of surface adsorbed cations on mica and/or organization of solvent in diffuse layers confined to the molecularly narrow enclosure. The observation of structural forces is not limited to force experiments using mica. They also appear in the swelling of clays and and are related to the lubrication of surfaces.

Figure 11 shows an example of structural forces observed between mica and a thin silver film deposited on mica [7]. The solvent is octamethylcyclotetrasiloxane, OMCTS, a nonpolar liquid that consists of a quasi-spherical molecule with a mean molecular diameter of 8 Å. The force curve is qualitatively similar to that observed between two bare mica surfaces separated by OMCTS and other nonpolar liquids, demonstrating the extreme smoothness of the metal layer. A decaying oscillatory force is observed as a function of distance separating the surface, with a periodicity equal to the molecular diameter of OMCTS. A similar oscillatory function is often, but not always, observed for bare mica separated by aqueous solutions [Fig. 1] although the periodicity is reduced to 2.4 Å, corresponding to the mean diameter of H_2O.

The correlation between the periodicity of the force oscillations with the molecular diameter of the liquid molecule suggests that
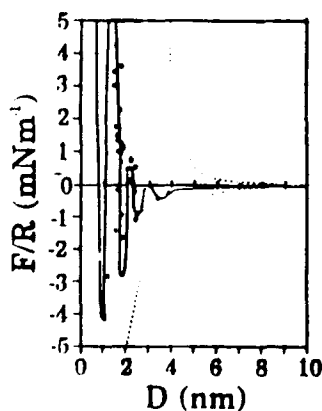

Figure 11. *Oscillatory force curve between Ag and mica separated by OMCTS. (From Reference 7, with permission.)*

confinement of a liquid between two surfaces results in a layering of the fluid molecules. This structural effect is very short ranged, limited to separations of several molecular diameters, as indicated by the rapid decay in the oscillations. The layering of the solvent does not appear to involve, at least in the case of nonpolar liquids, specific chemical interactions with the surfaces.

Observations of structural liquid layering between mica surfaces are relatively recent and are not completely understood. These interactions cannot be described by a continuum fluid theory. The oscillations reflect the graininess of the liquid, and one expects that successful models will take into account molecular instead of bulk properties of the liquid. A simplified explanation, for instance, uses a space filling model [43] to account for the density of spherical molecules such as OMCTS entrapped between the mica surfaces [Fig. 12]. At separations that allow close packing of the spheres (corresponding to integral values of the molecular diameter), the density of the fluid will be greatest. At any other separation distance, the average fluid density will fall below the bulk value. Thus, as the wall
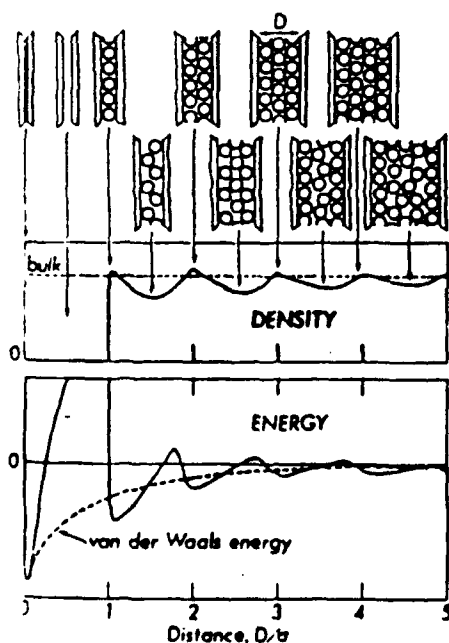

Figure 12. *Schematic diagram of the layering of nonpolar spherical fluid molecules (e.g., OMCTS) between two flat walls. The coarseness of the fluid at the molecular scale produces maxima and minima in the density profile that occur at multiples of the molecular diameter, σ. The oscillating density profile resulting from this solvent layering leads to a measurable oscillating interaction energy and "quantized" fluid flow between two closely (D < 5-10 σ) separated mica layers. (From Reference 43 (a), with permission.)*

separation is varied, the van der Waals interactions occur across a liquid with a periodically rising and falling mean density, causing the forces to undergo a similar oscillation.

The structural forces observed in aqueous solutions are more complex and dependent on chemical interactions, i.e., adsorption, between solutes and the surface [44,45]. In addition to oscillatory forces that probably arise for similar reasons as described above, a monotonically decaying repulsive or attractive structural force is often observed on hydrophilic and hydrophobic surfaces, respectively. These forces are referred to in the literature as hydration and hydrophobic structural forces, and their origin is not completely resolved. As an example, we consider the work of Pashley and coworkers [45] on hydration forces observed between ionized mica in electrolyte solutions, which bears a resemblance to electrode interfaces. In this study, strong repulsive hydration forces were observed in solutions containing chloride salts of Li^+, K^+, Na^+, and Cs^+, resulting from electrostatic binding of the cation to the negatively charged surface. The evidence supporting this includes: (a) no hydration forces were observed in pure water; (b) the magnitude of forces increases with the hydration of the bound layer in the order: $Li^+ = Na^+ > K^+ > Cs^+$; and (c) the hydration forces are nearly independent of the concentration at high concentrations corresponding to saturation coverage. Pashley has used a mass-action law to describe the competitive surface binding of metal cations and H^+ (or H_3O^+) in order to explain the observed dependence on the cation concentration. These workers also concluded that the extra hydration force resulted from "dehydrating" the adsorbed metal cation in a multistep process as the surfaces were pushed together.

The structure of hydrated metal cations on mica, implied by force measurements, is analogous to the conceptual model of a Stern layer of ions adsorbed at a finite distance, δ, from the surface. The Stern layer model has been implicitly applied by Claesson et al. in analyzing force curves obtained in concentrated solutions of a series of tetraalkylammonium bromide salts [46] [Fig. 13]. In these measurements, the distance of closest approach of the two surfaces (defined by an apparent hard wall contact) corresponds to twice the molecular diameter of the large organic cation adsorbed on the mica surface. The DLVO theory gives a good fit to the data beyond a separation distance of 2δ assuming a plane of charge located at a distance δ from each surface.
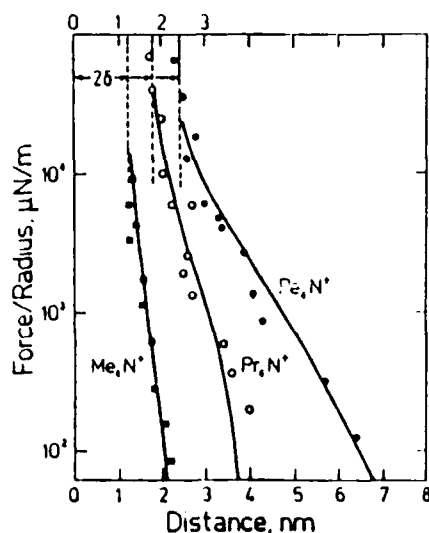
Figure 13. *Forces between mica as a function of distance in concentrated aqueous solutions of $R_4N^+Br^-$ salts. Me = methyl, Pr = propyl, and Pe = pentyl. The continuous curves assume a Stern layer of thickness δ that corresponds roughly to the thickness of the adsorbed cation. (From Reference 44. Copyright © 1985 Royal Swedish Academy. Reprinted with permission of Cambridge University Press.)*

The oscillatory and hydration forces directly observed through force measurements are related to other interfacial parameters of interest, which have been investigated by both experimental and computational methods, e.g., molecular dynamics [47,48]. One parameter, the effective molecular diffusivity in a pore (e.g., zeolite or polymer), has been indirectly related to transport limited rates measured at electrodes of nanoscopic dimensions [49]. Hydrodynamics in narrow enclosures have also been experimentally investigated by Chan and Horn [2] and Israelachvili [3], using transient force measurement techniques. In Chan and Horn's experiment, the lower mica surface is driven at a constant rate towards the upper surface. The hydrodynamic drag of the moving surface slows its movement, which is detected by interferometry using a video recording system and analyzed on the basis of Reynolds theory to, in effect, yield the liquid viscosity as a function of separation distance. An example of one experiment is shown in Figure 14, where the two surfaces were mica (in a crossed cylindrical orientation), and the liquid was OMCTS (qualitatively similar results have been obtained in liquid alkanes). At large separations (>50 nm), Chan and Horn found good quantitative agreement between theory and experiment, indicating that the viscosity within this region is equal to the bulk value. At shorter distances, the rate of the movement of the lower

surface was slower than predicted, indicating an increase in viscosity. The magnitude of this increase is small, but the values are experimentally significant. A more interesting behavior is observed at distances less than 2 nm. In this regime, the movement of the lower surface is no longer a monotonic function of time, but instead occurs in a jump-wise fashion, with the size of each jump equal to the mean diameter of OMCTS. Further, the
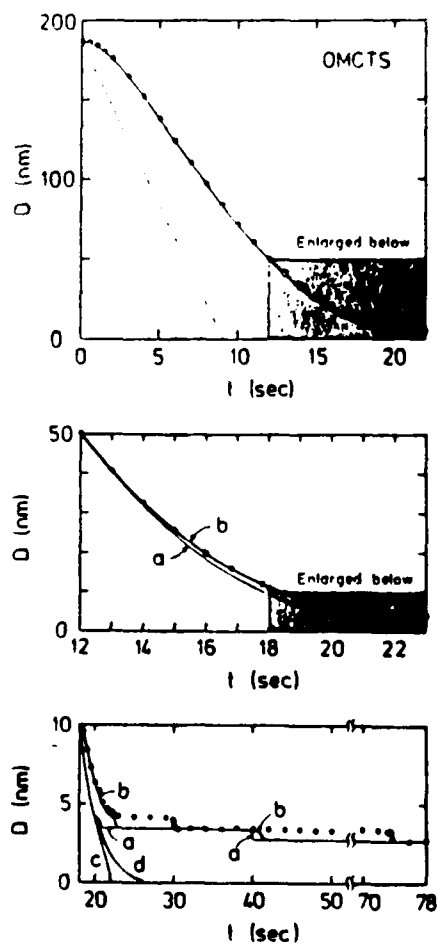

Figure 14. *Plot of the rate of drainage between two mica sheets immersed in OMCTS. In this experiment, one of the mica surfaces is driven at a constant rate, 20.5 nm/s, towards the opposing surface. The open circles represent the measured distance between the surfaces as a function of time. The top frame shows the measured distance as a function of time (the surface separation is 185 nm at t = 0 s) and the predicted response (solid line) based on Reynolds theory for hydrodynamic flow. The middle frame shows the same quantities for distances below 50 nm and at longer times where there is a small but significant deviation between the experiment and theory, indicating an increase in the apparent fluid viscosity. At very small separations (< 5 nm), bottom frame, OMCTS molecules flow out between the surfaces in a series of discrete jumps. The jump size is 0.75 nm, which corresponds to the OMCTS molecular diameter. Solid curves labeled (a)-(d) are theoretical predictions described in the original report. (From Reference 2, with permission.)*

time interval between jumps becomes progressively longer with each jump, indicating that the fluid is becoming progressively more difficult to squeeze out. This type of flow is indicative of the ordering of fluid molecules that can be obtained in narrow pores.

V. FORCES BETWEEN POLYMER FILMS

Several groups have extended the use of the surface forces apparatus to the study of adsorbed polymers [13-16]. Knowing the intermolecular forces that occur between polymer layers and substrates and how these forces are affected by temperature, solvent, and so forth, can provide clues to predict polymer conformations on solid substrates.

Klein measured both the forces [13] between adsorbed polystyrene on mica in cyclohexane and the refractive index n of the medium between the two surfaces as a function of separation distance [Fig. 15]. Refractive index measurements allow the volume fraction of polymer between the surfaces to be estimated. The force diagram shows attractive van der Waals forces starting at a separation distance of ca. 65 nm and an attractive minimum at 20 nm. Compression below 20 nm leads to a repulsive force. The results can be qualitatively explained in terms of the phase behavior for polystyrene in cyclohexane [Fig. 16]. In the region where there are no measurable forces ($D > 65$ nm), the polymer layers are not yet in contact, and the measured refractive index n corresponds to that of bulk cyclohexane. With a decrease in D, the effective polymer volume fraction in the region where the chains overlap, ϕ_{OV}, increases and leads to a two phase system with reduced free energy. This is experimentally seen as an attractive well in the force curve and an increase in the refractive index. When the compression increases past ϕ_2, a one phase region again exists. In this region, compression causes the chain density to increase and, thus, the free energy to increase. The configurational entropy of the polymer between the mica surfaces also decreases in this region, contributing to the repulsive part of the force-distance curve experimentally observed.

Force measurements have been made by Hadziioannou et al. [15] on block copolymers of poly(vinyl-2-pyridine)/polystyrene (PV2P/PS). The PV2P segment of the polymer is adsorbed in a flattened configuration on the mica surfaces; the PS segment is
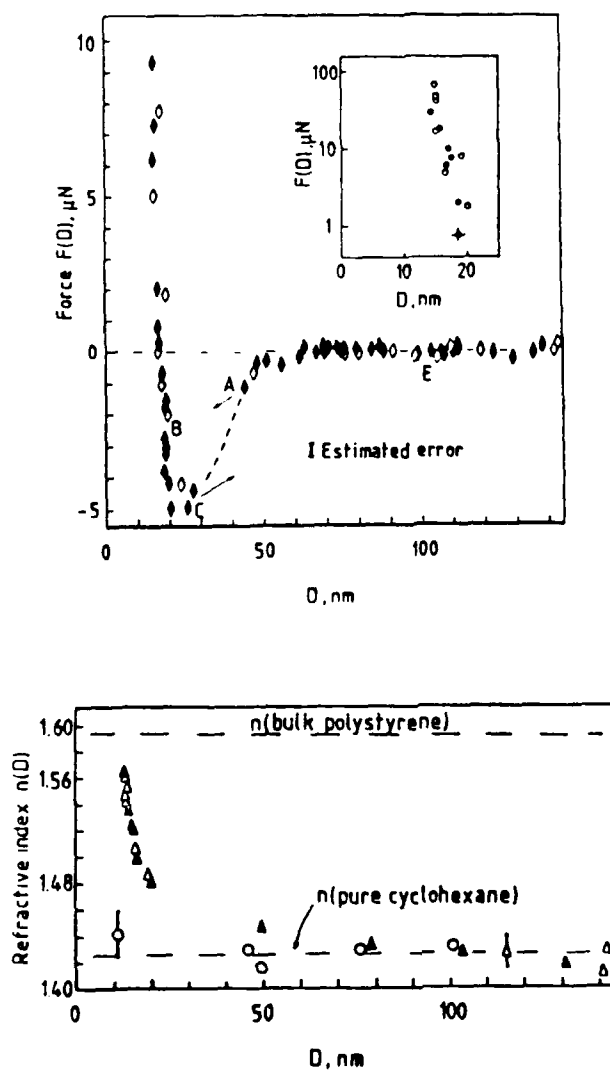
Figure 15. *(top) Forces between adsorbed polystyrene on mica in cyclohexane; (bottom) Refractive index of adsorbed polystyrene on mica as a function of surface separation. (From Reference 13 (a), with permission.)*
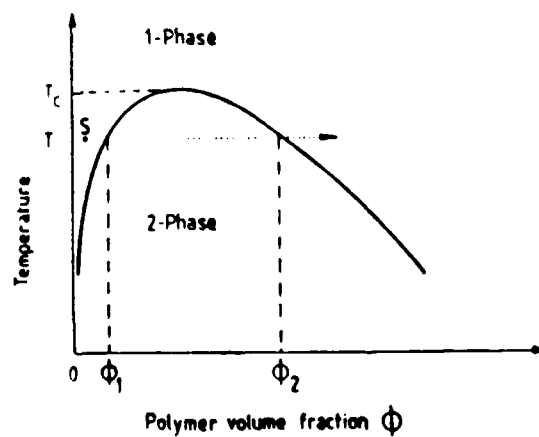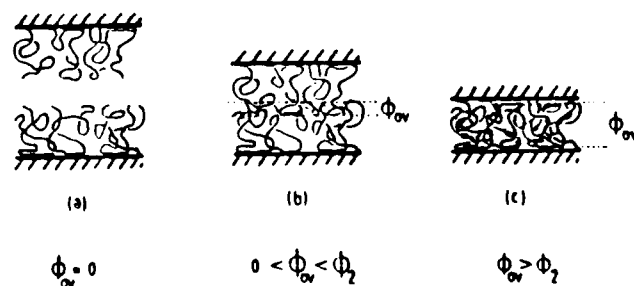
Figure 16. *(top) Schematic showing the overlap of the polystyrene layers as a function of surface separation; (bottom) The equilibrium phase diagram for polystyrene in cyclohexane. (From Reference 13 (a), with permission.)*

covalently bound to the PV2P segment and is oriented towards the solution phase. This configuration eliminates the possibility of the individual PS macromolecules bridging the gap and adsorbing directly on mica. (The bridging configuration is thought to cause additional attraction in the case of the adsorbed PS homopolymer). In a good solvent such as toluene, the PS chains are in an extended configuration away from the surface, and compression of the surfaces causes an overlap of the PS chains as previously. The subsequent repulsion observed for the block copolymer, however, begins at $10\ R_g$ (where R_g is the radius of gyration of the polymer), as compared to the $3\ R_g$ of homopolystyrene. Changing the solvent to cyclohexane substantially reduces the repulsive range to about $4\ R_g$. This reduction of the repulsive range is due to the configurational contraction of the PS chains and a decrease of the binary interactions between the polymer segments. Use of the copolymer allows observation of the thermodynamic segmental interaction between the PS layers without the added attractive contribution due to bridging. The authors also measured an increase in the onset of repulsive forces with increasing molecular weight of the polystyrene [Fig. 17]. They attribute this to terminally attached and extended polystyrene chains, which form a layer of uniform density whose thickness increases with the molecular weight of the polystyrene block.

VI. ULTRA-THIN-LAYER ELECTROCHEMISTRY

In a unique application, Bard and coworkers have employed a modified surface forces apparatus to construct a dual-electrode thin-layer electrochemical cell where the spacing between working electrodes can be varied from tens of microns to less than 1 nm. In these experiments, the surface forces apparatus is used to control the separation between two Pt or highly oriented pyrolytic graphite (HOPG) electrodes, oriented in a crossed cylindrical geometry, while monitoring forces and/or faradaic currents between the electrodes [19,50,51]. In a typical experiment, one electrode is biased at a potential to effect the oxidation (or reduction) of a soluble redox species, e.g., $Fe(CN)_6^{-4} \rightarrow Fe(CN)_6^{-3} + e^-$, which diffuses across the gap where it is rereduced (or reoxidized) at the second electrode. The electrochemical cell circuit is similar to that of conventional dual-electrode cells, allowing steady-state and transient electrochemical
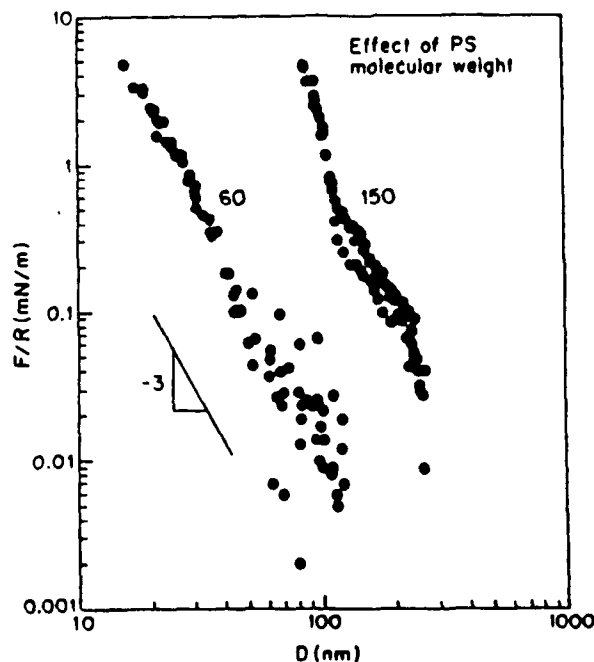
Figure 17. *Log-log plot of the force versus distance curve for two molecular weights (60,000 MW and 150,000 MW) of PS in the block copolymer PV2P/PS adsorbed on mica. (Reprinted with permission from Reference 15. Copyright © 1986 American Chemical Society.)*

measurements to be performed. Of interest is the fact that the electrode gap can be reduced to essentially molecular dimensions, allowing processes to be investigated that would not be possible in a conventional cell. For instance, in experiments with the $Fe(CN)_6^{-4/-3}$ couple, Fan and Bard [50] found that the current-distance behavior between two Pt electrodes could be separated into three regimes: (a) at large separations, $D > 300$ Å, the steady-state current could be accounted for by normal diffusional transport of the electroactive species across the gap, taking into account the crossed cylindrical electrode geometry; (b) at intermediate distances ($10 < D < 300$ Å), the current is somewhat

larger than expected for a mass-transport controlled reaction, indicating that new factors, such as an altered reactant concentration resulting from double-layer electrostatic forces or a change in fluid viscosity near the electrode surfaces, are effecting the transport controlled rate; and (c) at short distances ($D < 10$ Å), the current shows a nearly exponential increase with decreasing distance suggesting electron tunneling directly between the two surfaces. In the same paper, these authors also demonstrated electron-transfer between two redox active polymer coated Pt electrodes as the surfaces were brought into contact.

In an experiment combining faradaic electrochemistry and surface force measurements, Lee and Bard [19] measured the adhesion forces between unactivated and activated HOPG surfaces immersed in aqueous Na_2SO_4 and correlated their findings with the activation kinetics observed for $K_3Fe(CN)_6$ reduction on the same surfaces. The adhesion force for unactivated (hydrophobic) HOPG in the aqueous solution was found to be approximately equal to the value measured in air (50 μN), indicating little hydration of the unactivated surface. Activated HOPG, produced by pulsing the electrode potential between 1.5 V and -1.5 V vs SCE, resulted in a dramatic decrease in the adhesion force (2 μN) and a marked increase in rate of $Fe(CN)_6^{-3}$ reduction. Both effects were ascribed to the more hydrophilic nature of the activated surface.

VII. CONCLUSIONS

The selected experimental results presented in this chapter demonstrate how detailed pictures of interfacial structure can be obtained from force measurements. Although the majority of past work has dealt with forces between mica surfaces, it appears feasible to make similar measurements with electrodes of smoothness comparable to that of mica. The technical problems in preparing ultra-smooth electrode surfaces are obvious, but not insurmountable. Materials such as HOPG [19] and layered compound semiconductors (e.g., WSe_2) are natural candidates, as they can be cleaved to obtained molecularly smooth surfaces. The deposition of solid and liquid metal thin films, while providing a greater range of materials for study, will be more technically demanding in their preparation.

The very high resolution and sensitivity of the surface forces apparatus allows interfacial structure to be probed over distances

which range from the size of a macromolecule to the thickness of the Helmholtz plane. It should be possible to extract similar detailed information on a myriad of structures with dimensions intermediate between these extreme cases. Force measurements appear particularly well suited for in situ studies of modified electrodes (e.g., thin oxide coatings and organic films), simultaneously providing molecular structure, e.g., orientation and coverage, and the potential distribution across these interfaces. The most fundamental and direct information of double-layer structure and ion adsorption has been obtained from force measurements by investigators whose primary interests concern colloid chemistry. There are, however, a rich variety of questions regarding double-layer structure at metal electrodes that have yet to be explored by a direct experimental technique. As an example, the dependence of structural or hydration forces at metal surfaces, where the electronic charge is uniformly smeared out (vs localized ionic charge on mica), has not been measured. Forces at metals can be made over a wide range of potentials and charges not available using mica, extending our knowledge of double layer phenomena.

The ability to perform chemistry between surfaces separated by an inter-electrode gap of nanometers or less, as in the initial *studies* by Bard and coworkers, makes possible new types of experiments to explore chemical dynamics. For instance, one can imagine using the surface forces apparatus to measure the electron transfer rate as a *function of distance* (with angstrom resolution) between redox species immobilized on the two surfaces or to measure the distance dependence of energy transfer between a luminescent polymer and a metal surface. These exciting possibilities await further development, but are likely to provide new insights into chemistry occurring at interfaces.

References

1. Israelachvili, J. N., and Adams, G. E. *J. Chem. Soc. Faraday Trans. 1* 74 (1978): 975.
2. Chan , D. Y. C., and Horn, R. G. *J. Chem. Phys.* 83 (1985): 5311.
3. Israelachvili, J. N., *J. Colloid and Interface Sci.* 110 (1986): 263.
4. Pashley, R. M., and Israelachvili, J. N. *J. Colloid and Interface Sci.* 101 (1984): 511.
5. Christenson, H. K.; Horn, R. G.; and Israelachvili, J. N. *J. Colloid and Interface Sci.* 88 (1982): 79.
6. McGuiggan, P. M., and Pashley, R. M. *J. Phys. Chem.* 92 (1988): 1235.
7. Parker, J. L., and Christenson, H. K. *J. Chem. Phys.* 88 (1988): 8013.
8. Israelachvili, J. N. *Intermolecular and Surface Forces.* London: Academic Press, 1985.
9. Claesson, P. M. and Christenson, H. K. *J. Phys. Chem.* 92, (1988): 1650.
10. Israelachvili, J. N., and Pashley, R. M. *J. Colloid and Interface Sci.* 98 (1984): 500.
11. Pashley, R. M. et al. *Science* 229 (1985): 1088.
12. Israelachvili, J. N.; McGuiggan, P. M.; and Homola, A. M. *Science* 240 (1988): 248.
13. (a) Klein, J. *Adv. Colloid and Interface Sci.*, 16 (1982): 101; (b) Klein, J. *Nature*, 288 (1980): 248.
14. Israelachvili, J. N., et al. *Macromolecules* 17 (1984) 204.
15. Hadziioannou, G., et al. *Am. Chem. Soc.* 108 (1986): 2869.
16. Marra, J., and Hair, M. L. *J. Phys. Chem.* 92 (1988): 6044.
17. Smith, C. P., et al. *J. Ph   hem.* 92 (1988): 199.
18. van Blokland, P. H. G. M   and Overbeek, J. T. *J. Chem Soc., Faraday Trans. 1* 74 (1978)· 26 7.
19. Lee, C.-W., and Bard, A. J. *J. Electrochem. Soc.* 135 (1988): 1599.
20. Binning, G., ar J Rohrer, H. *Helv. Phys. Acta* 55 (1982): 726.
21. Christenson, H. K. *J. Phys. Chem.* 90 (1986): 4.
22. McGuiggan, P. M., and Israelachvili, J. N. *Chem. Phys. Lett.* 149 (1989): 469.
23. Israelachvili, J. N., and McGuiggan, P. M. *Science* 241 (1988): 795.
24. Tolansky, S. *Multiple Beam Interferometry.* Oxford: Clarendon Press, 1948.
25. Vanderlick, T. K. *Ph.D. Thesis.* Minneapolis: University of Minnesota, 1988.
26. Derjaguin, B. V., et al. *J. Colloid Sci.* 19 (1964): 113.
27. (a) Derjaguin, B. V. *Kolloid-Z.* 69 (1934): 155; (b) Barouch, E.; Matijevic, E.; and Parsegian, V. A. *J. Chem. Soc., Far. Trans. 1* 82 (1986): 2801.
28. Israelachvili, J. N. *J. Colloid and Interface Sci.* 44 (1973): 259.
29. Clarkson, M. T. *J. Phys. D: Appl. Phys.* 22 (1989) 475.
30. Derjaguin, B. V., and Landau, L. *Acta Physicochem. URSS* 14 (1941): 633.
31. Verwey, E. J. W., and Overbeek, J. T. G. *Theory of the Stability of Lyophobic Colloids.* Elsevier: Amsterdam, 1948.
32. Voropajeva, T.; Derjaguin, B.; and Kabanov, B. *Compt. Rend. Acad. Sci. U.R.S.S.* 128 (1959) 981.
33. Frumkin, A. N. *J. Electrochem. Soc.* 107 (1960): 461.
34. Tabor, D., and Winterton, R. H. S. *Nature* 219 (1968): 1120.
35. Israelachvili, J. N., and Adams, G. E. *Nature* 262 (1976): 774.
36. Bard, A. J., and Faulkner, L. R. *Electrochemial Methods.* New York: Wiley, 1980.

37. Devereux, O. F., and de Bruyn, P. L. *Interactions of Plane-Parallel Double Layers.* Massachusetts: M.I.T. Press, 1963.
38. Hiemenz, P. C. *Principles of Colloid and Surface Chemistry,* 2nd ed., 12.7. New York: Marcel Dekker, 1986.
39. Guldbrand, L., et al. *J. Chem. Phys.* 80 (1984): 2221.
40. Scott, E. R.; White, H. S.; and McClure, D. J. *J. Phys. Chem.* 93 (1989): 5249.
41. Chan, D. Y. C.; Pashley, R. M.; and White, L. R. *J. Colloid and Interface Sci.* 77 (1980): 283.
42. For recent advances in this field, see the Proceedings from the Conference on "Hydration Forces and Molecular Aspects of Solvation." (Orenas, Sweden, June 1984), *Chemica Scripta* 25 (1985): 1.
43. (a) Israelachvili, J. N. *Adv. Colloid and Interface Sci.* 16 (1982): 31. (b) Ninham, B. N. *J. Phys. Chem.* 84 (1980): 84.
44. Israelachvili, J. N. *Chemica Scripta* 25 (1985): 7.
45. Pashley, R. M. *Chemica Scripta* 25 (1985): 22.
46. Claesson, P.; Horn, R. G.; and Pashley, R. M. *J. Colloid and Interface Sci.* 100 (1984): 250.
47. Bitsanis, I., et al. *J. Chem. Phys.* 89 (1988): 3152.
48. Davis, H. T., et al. *ACS Symposium Series No. 353, Supercomputer Research in Chemistry and Chemical Engineering,* ed. K. F. Jensen and D. G. Truhlar, 1987.
49. Morris, R. B.; Franta, D. J.; and White, H. S. *J. Phys. Chem.* 91 (1987): 3559.
50. Fan, F.-R. F., and Bard, A. J. *J. Am. Chem. Soc.* 109 (1987): 6262.
51. Davis, J. M.; Fan, F.-R. F.; and Bard, A. J. *J. Electroanal. Chem.* 238 (1987): 9.